In Situ Polymerization and Photophysical Properties of Poly(*p*-phenylene benzobisoxazole)/Multiwalled Carbon Nanotubes Composites

Chengjun Zhou,[1,2] Xueying Qiu,[1] Qixin Zhuang,[1] Zhewen Han,[1] Qinglin Wu[2]

[1]*Key Laboratory for Specially Functional Polymeric Materials and Related Technology of the Ministry of Education, School of Materials Science and Engineering, East China University of Science and Technology, Shanghai 200237, China*
[2]*School of Renewable Natural Resources, Louisiana State University Agricultural Center, Baton Rouge, Louisiana 70803*

Received 18 May 2011; accepted 24 August 2011
DOI 10.1002/app.35532
Published online 6 December 2011 in Wiley Online Library (wileyonlinelibrary.com).

ABSTRACT: Poly(*p*-phenylene benzobisoxazole)/multiwalled carbon nanotubes (PBO-MWCNT) composites with different MWCNT compositions were prepared through *in situ* polymerization of PBO in the presence of carboxylated MWCNTs. The nanocomposite's structure, thermal and photophysical properties were investigated and compared with their blend counterparts (PBO/MWCNT) using Fourier transform infrared spectra, Raman spectra, Wide-angle X-ray diffraction, thermogravimetric analysis, UV-vis absorption, and photoluminescence. The results showed that MWCNTs had a strong interaction with PBO through covalent bonding. The incorporation of MWCNTs increased the distance between two neighboring PBO chains and also improved the thermal resistance of PBO. The investigation of UV-vis absorption and fluorescence emission spectra exhibited that *in situ* PBO-MWCNT composites had a stronger absorbance and obvious trend of red-shift compared with blend PBO/MWCNT composites for all compositions. This behavior can be attributed to the efficient energy transfer through forming conjugated bonding interactions in the PBO-MWCNT composites. © 2011 Wiley Periodicals, Inc. J Appl Polym Sci 124: 4740–4746, 2012

Key words: poly(*p*-phenylene benzobisoxazole) (PBO); multiwalled carbon nanotubes (MWCNTs); nanocomposites; *in situ* polymerization; photophysical properties

INTRODUCTION

As polymer-carbon nanotubes (polymer/CNT) composites were first reported in 1994 by Ajayan et al.,[1] they have become a subject of intensive research and technological development with the hope of delivering CNTs' superior mechanical and/or electrical properties to polymeric materials for various targeting applications, including the area of electrical appliances and the aircraft and automotive industries.[2,3] However, because of their high aspect ratio and strong inter-tube van der Waals forces, CNTs often aggregate in the matrix. In addition, the chemical inertness of CNTs weakens greatly the interface between CNTs and polymer matrix. Hence, the dispersion of CNTs and the polymer-CNT interfacial adhesion has become two of the most important issues to limit their practical applications. For solving the two problems, various strategies and approaches have been adopted. Among these approaches, surface modification of CNTs has been intensively studied as an efficient way to improve stable and uniform dispersion of CNTs and the polymer/CNT interfacial adhesion in the composites.[4] Currently, covalent and strong noncovalent attachments are two main options to modify CNTs.[5] Because the covalent attachment is permanent and mechanically stable, it can provide a stronger linkage between CNTs and matrix in comparison with the noncovalent attachment.[6]

Poly(*p*-phenylene benzobisoxazole) (PBO) has received great attention because of its fully conjugated rod-like backbone entailing excellent mechanical properties, thermo-oxidative stability, and solvent resistance. PBO fibers registered under the trademark Zylon® are known to possess the highest tensile modulus and strength among all commercial synthetic polymer fibers.[7–9] However, only about 15% of the theoretical tensile strength has been achieved in the commercialized PBO fibers attributed to the low-molecular length (about 200 nm for fiber spinning) and defects.[10] To fully exploit the mechanical properties of PBO, several studies have been made on PBO/CNT composites to take

Correspondence to: Q. Zhuang (qxzhuang@ecust.edu.cn) or C. Zhou (czhou@agcenter.lsu.edu).

Contract grant sponsor: National Natural Science Foundation of China (NSFC); contract grant number: 50973028.

advantage of longer length of CNTs compared with that of PBO molecular chains.[11–15] These earlier reported PBO/CNT composites were mostly prepared by using *in situ* polymerization of PBO with modified CNTs for forming the covalent attachment between CNTs and PBO,[12,13,15] and there is indeed a remarkable improvement in the mechanical properties. However, the other properties of the covalent PBO/CNT composite have not yet been fully investigated except that the conductivity of PBO/hydroxyamide grafted CNT composite fibers was reported in our previous article.[13] Considering CNTs also exhibit special optical behavior in addition to excellent electrical conductivity as well as superb mechanical properties,[16] this study concerning the photophysical properties of PBO/CNT nanocomposites can help explore the effect of incorporated CNTs on the optical properties of PBO to expand potential of PBO used as high performance materials in optoelectronic displays and aerospace fields.[17,18]

In this article, PBO-MWCNT composites with different compositions of carboxylated multiwalled carbon nanotubes (C-MWCNTs) were prepared by using *in situ* polymerization of PBO. The dispersion and interfacial adhesion of CNTs in the PBO-MWCNT composite fibers were characterized. The thermal resistance of *in situ* PBO-MWCNT composites was also evaluated. Moreover, the photophysical properties of PBO-MWCNT composites were investigated in thin films and compared with their blend counterparts for understanding the effect of the attachment method of CNTs on the photophysical properties of PBO-MWCNT composites.

EXPERIMENTAL

Materials

One monomer for polymerizing PBO, 4,6-diaminoresorcinol dihydrochloride (DAR·2HCl), was synthesized in our laboratory according to the previous reports.[19,20] Another monomer terephthalic acid (TPA) was purchased from Shanghai Reagents Co. (Shanghai, China) and dried before use. Methanesulfonic acid (MSA) was purchased from Sigma-Aldrich Corporation. Phosphoric acid (H_3PO_4), phosphorus pentoxide (P_2O_5), and poly(phosphoric acid) (PPA) with a P_2O_5 content of 70.7 weight percentage (wt %) were purchased from the Shanghai Sinopharm Chemical Reagent Co. (Shanghai, China) and were used as received. Pristine MWCNTs with an average diameter of $\sim$ 30 nm was provided from Tsinghua-Nafine Nano-Powder commercialization engineering center (Beijing, China). Carboxylated MWCNTs (C-MWCNTs) was prepared as described in our earlier report.[14] Briefly, MWCNTs were treated by a 65% HNO_3 aqueous solution with the ultrasonication for 30 min and the reaction for 20 h at 90°C, and then were filtered, washed, and dried. The blend nanocomposites of PBO with C-MWCNTs (PBO/MWCNT) were also fabricated according to our earlier report.[14]

In situ polymerization of PBO-MWCNT composites

Viscous solutions of PBO or *in situ* PBO-MWCNT composites in PPA were prepared using the polycondensation[13,21–25] of DAR·2HCl and TPA with or without C-MWCNTs. The compositions of C-MWCNTs were 1 and 5 wt % with respect to the weight of PBO. The corresponding composites were designated as *in situ* PBO-MWCNT-1% and 5%, respectively. For simplicity, a hyphen "-" and a forward slash "/" are used between PBO and MWCNT to stand for *in situ* and blend composites, respectively. For example, *in situ* composite with 1 wt % C-MWCNTs was designated as *in situ* PBO-MWCNT-1%, whereas the blend composite with 1 wt % C-MWCNTs was marked as blend PBO/MWCNT-1%. To illustrate the fabrication procedure of composites (Figure 1), the preparation of *in situ* PBO-MWCNT-1% was described in detail as follows. A total of 20.245 g of PPA were loaded into a 250 mL glass vessel equipped with a mechanical stirrer and nitrogen inlet/outlet; 5.000 g of DAR·2HCl and 3.899 g of TPA were added and mixed together with PPA at 90°C under a nitrogen atmosphere until complete removal of hydrochloride. A sample of 0.056 g of C-MWCNTs in 10 mL H_3PO_4 treated with ultrasonic bath (40 kHz) for 30 min was added to the mixture, and another 32.688 g of P_2O_5 was then added to bring the P_2O_5 concentration up to 85 wt % and result in a final polymer concentration of 14 wt %. The polymerizing mixture was first stirred under vacuum at 120°C for 8 h. It was then heated to 180°C stepwise at 5–10°C h^{-1}, and kept at this temperature for another 8 h with constant stirring. The obtained highly viscous dope was planished to film and was then dipped in a large volume of distilled water for at least 3 days to remove the PPA completely. The water bath was examined with pH paper till it became neutral. Finally, the polymer films were dried at 80°C in a vacuum oven for 24 h.

Characterizations and measurements

Fourier transform infrared (FTIR) spectra were taken on a Nicolet FTIR analyzer (Magna-IR550). Nanotubes were examined by using KBr disk method. Transmission FTIR spectra of PBO and composite films were obtained using sample-spread CaF_2 disks. The photos of PBO and *in situ* PBO-MWCNT composites dissolved in MSA (2 mg of samples in 1 mL

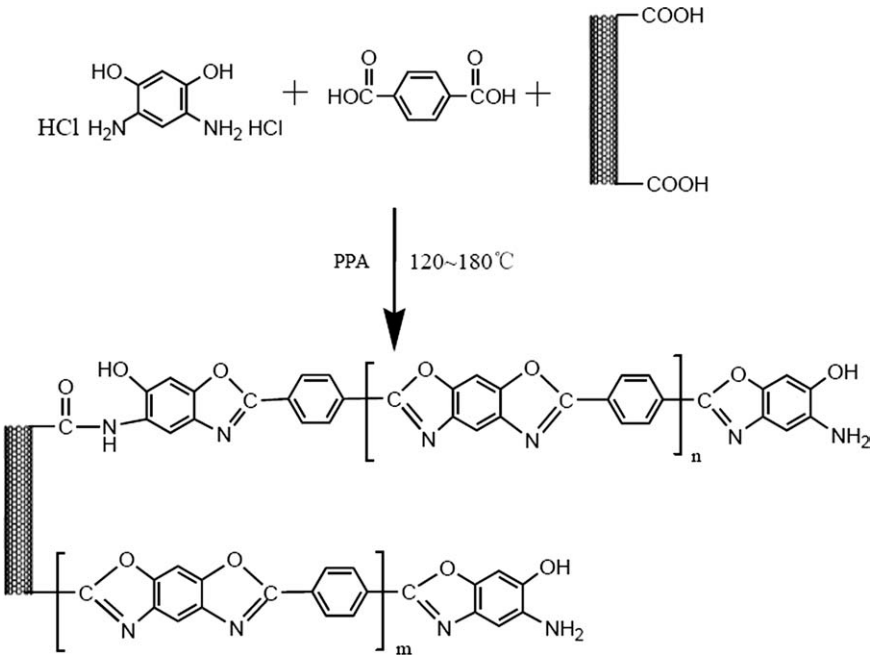

Figure 1 *In situ* polymerization of PBO-MWCNT composites.

solvent) were taken using a digital camera (Kodak, DSC-Z730). Wide-angle X-ray diffraction (WAXD) patterns were collected in a 2θ scan range of 5–40° on a Rigaku D/max-rB rotating anode X-ray generator with Ni-filtered CuKα ($\lambda = 0.15401$ nm) radiation operated at 100 mA and 40 kV. Raman spectra were collected at 514 nm excitation (He-Nelaser) on a Renishaw InVia Reflex Raman spectrometer in a backscattering configuration. Thermal stability of PBO and *in situ* PBO-MWCNT composites was investigated using a DuPont 1090B thermogravimetric analyst (TGA) at a heating rate of 10°C min^{-1} in a dynamic nitrogen environment. UV-vis absorption and photoluminescence (PL) of the polymer films were recorded on a Varian Cary 500 UV/Vis/NIR spectrophotometer and a Hitachi 850 fluorescence spectrophotometer at room temperature, respectively. Thin polymer films of good optical quality were prepared by using Jenekhe's method,[26] i.e., spin-coating of the polymer solution in nitromethane/$AlCl_3$ with a polymer concentration of 3 wt % onto synthetic silica substrates. The thin films were dried at 80°C in a vacuum oven for 12 h after complete decomplexation in deionized water for over 3 days. The intrinsic viscosities ([η]) of all the samples were measured in MSA at 30°C by using a modified device based on the Ubbelohde capillary viscometer.

RESULTS AND DISCUSSION

Structures characterization

[η] for PBO, *in situ* PBO-MWCNT-1%, and *in situ* PBO-MWCNT-5% in MSA at 30.0 ± 0.2°C were 5.0, 5.0, and 3.0 dL g^{-1}, respectively. Using a third-order least-squares regression equation for the correlation between [η] and the weight-average molecular weight (M_w) of PBO,[27] M_w of PBO for PBO, *in situ* PBO-MWCNT-1%, and *in situ* PBO-MWCNT-5% was calculated to be 2.2×10^4, 2.2×10^4, and 1.5×10^4 g mol^{-1}, respectively. This result suggested that the molecular weight of PBO in the nanocomposites with low content of MWCNTs was as high as that of pure PBO, but high loading of MWCNTs hindered the increase of molecular weight of PBO during *in situ* polymerization of PBO-MWCNT composites. This is because that the incorporation of MWCNTs reduced the chance of PBO chain combination, which results in the decrease of molecular weight of PBO in *in situ* PBO-MWCNT composites, especially with high MWCNT contents.

FTIR spectra of C-MWCNTs, PBO, and *in situ* PBO-MWCNT are shown in Figure 2. The spectrum of C-MWCNTs exhibited the C=O and —OH stretching modes of the carboxyl group at 1705 and 3100–3700 cm^{-1}, and C=C graphitic stretch in MWCNTs at 1560 cm^{-1}. PBO exhibited a broad absorption band at 3200–3600 cm^{-1} due to end-capped amino (N—H) and hydroxyl (—OH) groups. The characteristic peak at 1720 cm^{-1} for PBO assigned to the stretching vibration of —C=O in the end carboxylic groups diminished in the *in situ* PBO-MWCNT composites. In addition, a slightly characteristic peak at 1680 cm^{-1} attributed to amide group (—NHC(O)—) occurred after the incorporation of C-MWCNTs likely because of the incomplete cyclization reaction between PBO and C-MWCNTs.[28] As discussed in our previous studies on poly(benzazole)s,[29,30] this incomplete closure of the

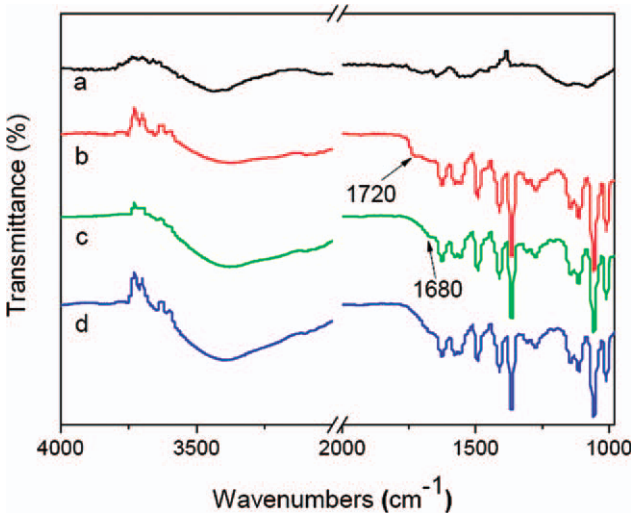

Figure 2 FTIR spectra of C-MWCNTs (a), PBO (b), *in situ* PBO-MWCNT-1% (c), and *in situ* PBO-MWCNT-5% (d) [Color figure can be viewed in the online issue, which is available at wileyonlinelibrary.com].

oxazole rings was attributed to the existence of residual phosphoric acid. These results suggested the covalent bonding between MWCNT and PBO *in situ* polymerization, as proposed in Figure 1. Moreover, the composites with different MWCNT compositions displayed no distinguishable difference in most band positions from those of the polymer matrix due to the C=C graphitic stretch in C-MWCNTs overlapping with the aromatic ring C=C stretch in PBO.

To further investigate the interaction between PBO and C-MWCNTs, the characterization of Raman spectra of C-MWCNTs, PBO, and *in situ* PBO-MWCNT-5% was performed and are shown in Figure 3. PBO displayed a strong peak at 1618 cm^{-1} (the vibration mode of the backbone *p*-phenylene ring) and other characteristic peaks at 930, 1170, 1277, 1306, and 1543cm^{-1}.[11] Consistent with an earlier report on carboxylated MWCNTs,[15] G peak at 1579 cm^{-1} and D peak at 1329 cm^{-1} in C-MWCNTs were attributed to the optically active in-plane E_{2g} vibration and the defects in CNTs, respectively. A strong fluorescence for the *in situ* PBO-MWCNT-5% composite was observed except that all characteristic PBO peaks were detected. It implies the existence of MWCNTs in the composite. However, D peak of C-MWCNTs was unobvious in the spectra of *in situ* PBO-MWCNT-5% nanocomposite. This likely suggests that the covalent bonding between C-MWCNTs and PBO mostly forms on the defects of C-MWCNTs, in which —COOH groups presented participate in polymerization and then cause the linkage of the C-MWCNTs to the polymer.[31]

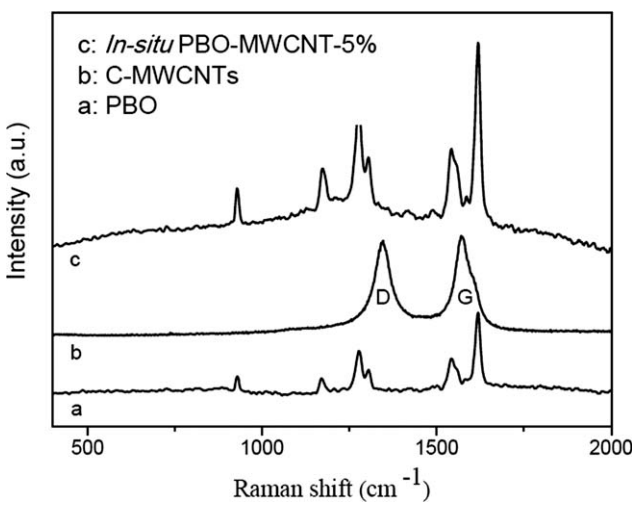

Figure 3 Raman spectra of PBO (a), C-MWCNTs (b), and *in situ* PBO-MWCNT-5% (c).

Figure 4 shows the photos of PBO, *in situ* PBO-MWCNT-1%, *in situ* PBO-MWCNT-5%, blend PBO/MWCNT-1%, and blend PBO/MWCNT-5% dissolved in MSA (2 mg mL^{-1}) after 48 h. From Figure 4, it can be seen that C-MWCNTs in blend PBO/MWCNT composites tend to aggregate in MSA after 48 h because of strong tube-tube van del Waal interactions. In contrast, *in situ* PBO-MWCNT composite demonstrated excellent solubility in MSA without obvious aggregations of MWCNTs and became gradually dark with increased C-MWCNTs contents, further suggesting that PBO was covalently grafted onto the carbon nanotubes and then limited the aggregation of C-MWCNTs.

TGA thermograms of pure PBO and *in situ* PBO-MWCNT composites are shown in Figure 5. Both PBO and *in situ* PBO-MWCNT composites exhibited an outstanding thermal stability with no appreciable weight loss up to 600°C. The on-set thermal degradation temperature (T_d) was defined as the intersection of tangents drawn from TGA curves. T_d of *in situ* PBO-MWCNT composites increased from 665°C for PBO to 681 and 685°C for PBO-MWCNT-1% and PBO-MWCNT-5%, respectively. This suggests that *in situ* PBO-MWCNT composites possessed a

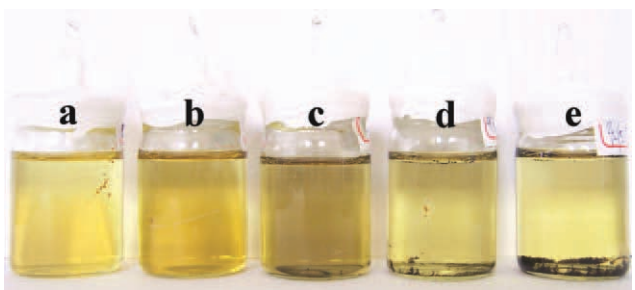

Figure 4 Photograph of PBO (a), *in situ* PBO-MWCNT-1% (b), *in situ* PBO-MWCNT-5% (c), blend PBO/MWCNT-1% (d), and blend PBO/MWCNT-5% (e) dissolved in MSA (2 mg mL^{-1}) after 48 h. [Color figure can be viewed in the online issue, which is available at wileyonlinelibrary.com].

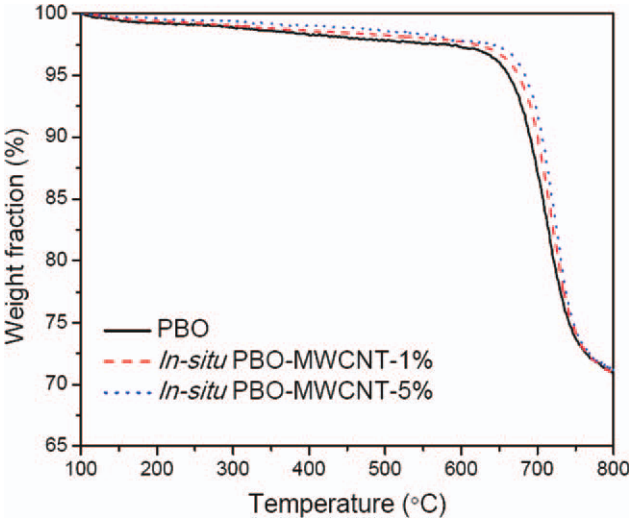

Figure 5 TGA thermograms of PBO, *in situ* PBO-MWCNT-1%, and *in situ* PBO-MWCNT-5% [Color figure can be viewed in the online issue, which is available at wileyonlinelibrary.com].

better thermal stability over PBO in N_2. In contrast with blend PBO/MWCNT composites,[14] *in situ* PBO-MWCNT exhibited slightly increased T_d at 1 wt % MWCNT content. Moreover, the residual weight at 800°C increased slightly with increasing the content of C-MWCNTs in the composites.

To investigate the effect of C-MWCNTs on the ordered structures of PBO matrix, WAXD patterns of *in situ* PBO-MWCNT-5% and blend PBO/MWCNT-5% films were measured, and the results are shown in Figure 6. In our previous reports,[14,24] pure PBO showed two major diffraction peaks at $2\theta = 16.28$ and 26.46° with respective to *d*-spacing of 0.544 and 0.336 nm, which stands for "side-by-side" distance on (200) plane and "face-to-face" distance on (010) plane between two neighboring PBO chains, respectively. From Figure 6, it can be seen that the (200) and (010) plane shifted to 15.92° (0.556 nm) and 26.10° (0.341 nm) for *in situ* PBO-MWCNT-5%, and 16.28° (0.544 nm) and 26.27° (0.339 nm) for blend PBO/MWCNT-5%. The result suggests that the incorporation of C-MWCNTs increased slightly the distance between two neighboring PBO chains for both nanocomposites. In addition, compared with *in situ* PBO-MWCNT-5%, blend PBO/MWCNT-5% showed two additional peaks at 13.87° and 25.13° attributed to the characteristic peak of MWCNTs.[32] This indicates that the dispersion of C-MWCNTs in blend PBO/MWCNT-5% was weaker than that of *in situ* PBO-MWCNT-5%.

Photophysical properties

The UV-Vis optical absorption properties of both *in situ* PBO-MWCNT and blend PBO/MWCNT composite films were investigated and the attenuation coefficient (α, also called extinction coefficient) are shown in Figure 7(a). α can be calculated by Beer's law, $T = 10^{-\alpha l}$, where T is the transmittance and l is the film thickness. The spectral data are summarized in Table I. The pure PBO film exhibited two major peaks at 403 nm (3.08 eV) and 429 nm (2.90 eV). These two major peaks were almost retained in both composites without obvious shift but progressively increased in the intensity with the increased concentration of C-MWCNTs in composites. This result is similar to Huang's report about PBO/MWCNT blend films.[17] Moreover, the absorbance intensity of *in situ* PBO-MWCNT composites was stronger than that of their blend counterparts for all compositions likely because of a better dispersion of MWCNTs in *in situ* PBO-MWCNT composites forming highly efficient absorbance. More importantly, unlike blend PBO/MWCNT composites, *in situ* PBO-MWCNT composites showed the peak intensity at 403 nm was stronger than the intensity at 429 nm, suggesting that there was strong interaction between C-MWCNTs and PBO in *in situ* PBO-MWCNT composites, as also reported for the *in situ* poly(2,5-benzoxazole)/carbon nanotube composites.[33] In addition, a remarkable trend of blue shift of absorption edge (λ_{onset}) with the increase of C-MWCNTs content can be observed in *in situ* PBO-MWCNT composites. It likely implies that there was observable ground-state energy transfer in the *in situ* nanocomposites through conjugated interactions between the aromatic PBO molecules and the nanotubes originated from the covalent bonding while it is ambiguous in the blend nanocomposites only through π-π stacking interactions between two components.

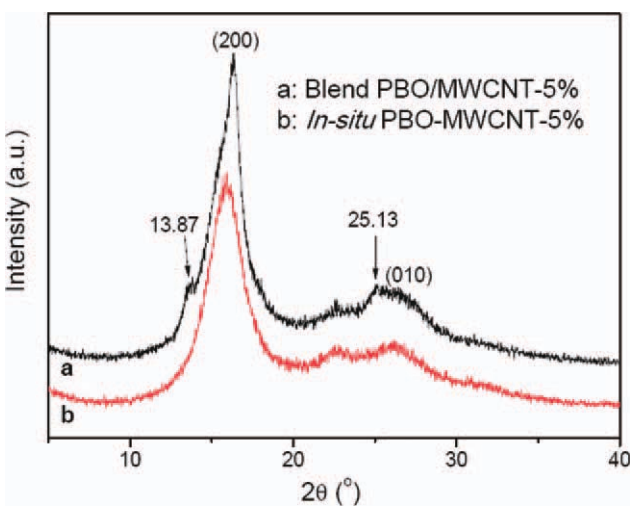

Figure 6 WAXD patterns of *in situ* PBO/MWCNT-5% (a) and blend PBO-MWCNT-5% (b) composites [Color figure can be viewed in the online issue, which is available at wileyonlinelibrary.com].

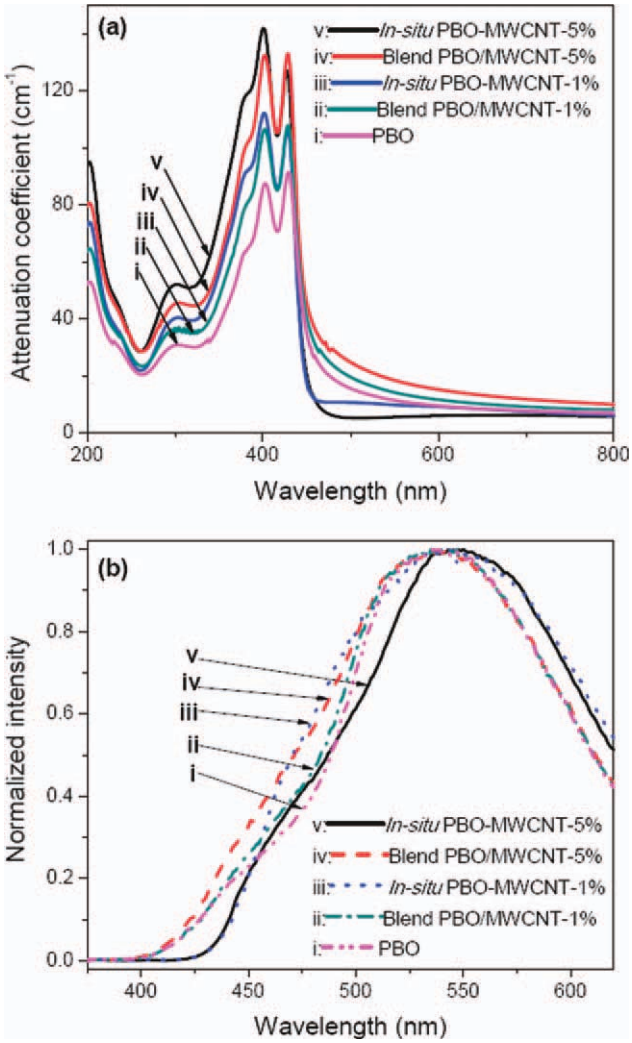

Figure 7 UV-vis absorption (a) and PL emission (b) spectra of PBO (i), blend PBO/MWCNT-1% (ii), *in situ* PBO-MWCNT-1% (iii), blend PBO/MWCNT-5% (iv), and *in situ* PBO-MWCNT-5% (v) films. [Color figure can be viewed in the online issue, which is available at wileyonlinelibrary.com].

The normalized PL emission spectra of PBO, *in situ* PBO-MWCNT, and blend PBO/MWCNT in thin films are shown in Figure 7(b). All films on a quartz substrate were excited at a wavelength of 325 nm.[17] The PL emission spectrum of PBO displays a broad and featureless peak with the maximum wavelength (λ_{max}) at 534 nm (2.33 eV), indicating yellow-green light emission. The PL spectrum of blend PBO/MWCNT composites showed similar peaks to that of PBO homopolymer, suggesting the fact that MWCNTs did not change the PBO lattice vibration and the optical band gap attributed to no intermolecular orbital interaction between PBO and MWCNTs in blend PBO/MWCNT composites.[17] From Figure 7(b) and Table I, it can also be seen that λ_{max} red-shifted to 539 nm (2.31 eV) for *in situ* PBO-MWCNT-1% and 550 nm (2.26 eV) for *in situ* PBO-MWCNT-5%, respectively. Thereby, the Stokes shifts between the emission and absorption maxima ($\Delta\lambda$) of *in situ* PBO-MWCNT composites are much higher (0.77 eV for PBO-MWCNT-1% and 0.84 eV for PBO-MWCNT-5%) than those of PBO and blend PBO/MWCNT composite (0.57 eV), as shown in Table I. Usually, $\Delta\lambda$ reflects the structural relaxation. $\Delta\lambda$ of PBO was attributed to the ring distortion and coplanar conformation of molecular chains.[21] As carbon nanotubes in excited state have the vibrational relaxation,[34] the incorporation of MWCNTs is expected to increase the Stoke shift of composites. The larger $\Delta\lambda$ of *in situ* PBO-MWCNT composites indicates that MWCNTs was excited to relax because of the effective energy transfer from PBO to MWCNTs through forming conjugated intermolecular interactions between two components. In addition, it should be pointed out that the original spectra (not shown) of *in situ* PBO-MWCNT composites before normalization as in Figure 7(b) are distinguished from those of PBO homopolymers and blend PBO/MWCNT composites by lower intensities of peak. The PL intensity dropped gradually with increasing the C-MWCNTs content, showing that the fluorescence of PBO can be quenched by MWCNTs. Similar fluorescence quenching was reported for Fluor-PEG-functionalized CNTs[35] and F-DMBN/CNTs composites[36] attributed to the energy transfer.

TABLE I
UV-vis Absorption and PL Emission Data of PBO, *In Situ* PBO-MWCNT Composite, and Blend PBO/MWCNT Composite Thin Films

Sample	Absorption λ (nm)		λ_{onset} (nm)	Emission λ_{max} (nm)	$\Delta\lambda$ (eV)
	λ_1	λ_2			
PBO	403	429[a]	458	534	0.57
In situ PBO-MWCNT-1%	402[a]	428	452	539	0.77
In situ PBO-MWCNT-5%	401[a]	428	449	550	0.84
Blend PBO/MWCNT-1%	402	429[a]	457	534	0.57
Blend PBO/MWCNT-5%	402	429[a]	456	533	0.57

[a] Maximum absorption wavelength (λ_{abs}); λ_{onset} is the onset of absorption edge; $\Delta\lambda$ is the Stokes shift between the emission and absorption maxima.

CONCLUSIONS

PBO-MWCNT composites were prepared using *in situ* polymerization of PBO in the presence of carboxylated MWCNTs. The investigation on the structures of *in situ* PBO-MWCNT composites demonstrated that there was a strong interaction between MWCNTs and PBO through covalent bonding. The incorporated C-MWCNTs increased the distance between two neighboring PBO chains and improved the thermal resistance of PBO. Interestingly, the optical absorbance and fluorescence of *in situ* PBO-MWCNT composites were distinctly different from those of blend PBO/MWCNT composites. *In situ* PBO-MWCNT composites displayed a stronger absorbance and obvious trend of red-shift compared with their blend counterparts for all compositions attributed to efficient energy transfer through the covalent bonding. This study explores the photophysical properties of PBO incorporated by covalently attached MWCNTs for further expanding potential applications of *in situ* PBO-MWCNT composites in high-performance articles through the excellent mechanical properties combined with the improved photo-stability.

References

1. Ajayan, P. M.; Stephan, O.; Colliex, C.; Trauth, D. Science 1994, 265, 1212.
2. Byrne, M. T.; Gun'ko, Y. K. Adv Mater 2010, 22, 1672.
3. Spitalsky, Z.; Tasis, D.; Papagelis, K.; Galiotis, C. Prog Polym Sci 2010, 35, 357.
4. Bose, S.; Khare, R. A.; Moldenaers, P. Polymer 2010, 51, 975.
5. Liu, P. Eur Polym J 2005, 41, 2693.
6. Kim, K. S.; Park, S. J. Macromol Res 2010, 18, 981.
7. So, Y. H. Prog Polym Sci 2000, 25, 137.
8. Kitagawa, T.; Yabuki, K.; Young, R. J. Polymer 2001, 42, 2101.
9. Davies, R. J.; Eichhorn, S. J.; Riekel, C.; Young, R. J. Polymer 2004, 45, 7693.
10. Chae, H. G.; Kumar, S. J Appl Polym Sci 2006, 100, 791.
11. Kumar, S.; Dang, T. D.; Arnold, F. E.; Bhattacharyya, A. R.; Min, B. G.; Zhang, X. F.; Vaia, R. A.; Park, C.; Adams, W. W.; Hauge, R. H.; Smalley, R. E.; Ramesh, S.; Willis, P. A. Macromolecules, 2002, 35, 9039.
12. Li, J. H.; Chen, X. Q.; Li, X.; Cao, H. L.; Yu, H. Y.; Huang, Y. D. Polym Int 2006, 55, 456.
13. Zhou, C. J.; Wang, S. F.; Zhang, Y.; Zhuang, Q. X.; Han, Z. W. Polymer 2008, 49, 2520.
14. Zhou, C. J.; Wang, S. F.; Zhuang, Q. X.; Han, Z. W. Carbon 2008, 46, 1232.
15. Li, X.; Huang, Y. D.; Liu, L.; Cao, H. L. J Appl Polym Sci 2006, 102, 2500.
16. Ajayan, P. M.; Zhou, O. Z. Carbon Nanotubes 2001, 80, 391.
17. Huang, J. W.; Bai, S. J. Nanotechnology 2005, 16, 1406.
18. Fu, Q.; Liu, X.; Zhuang, Q.; Qian, J.; Han, Z. Adv Mater Res 2011, 183–185, 201.
19. So, Y. H.; Heeschen, J. P.; Bell, B.; Bonk, P.; Briggs, M.; DeCaire, R. Macromolecules 1998, 31, 5229.
20. Xu, X. H.; Liu, X. Y.; Zhuang, Q. X.; Han, Z. W. J Appl Polym Sci 2010, 116, 455.
21. Wang, S. F.; Wu, P. P.; Han, Z. W. Macromolecules 2003, 36, 4567.
22. Wang, S. F.; Wu, P. P.; Han, Z. W. J Mater Sci 2004, 39, 2717.
23. Wang, S. F.; Guo, P. Y.; Wu, P. P.; Han, Z. W. Macromolecules 2004, 37, 3815.
24. Chen, Y.; Wang, S. F.; Zhuang, Q. X.; Li, X. X.; Wu, P. P.; Han, Z. W. Macromolecules 2005, 38, 9873.
25. Wang, S. F.; Chen, Y.; Zhuang, Q. X.; Li, X. X.; Wu, P. P.; Han, Z. W. Macromol Chem Phys 2006, 207, 2336.
26. Jenekhe, S. A.; Johnson, P. O. Macromolecules 1990, 23, 4419.
27. Roitman, D. B.; Wessling, R. A.; Mcalister, J. Macromolecules 1993, 26, 5174.
28. Wang, S. F.; Bao, G. B.; Lu, Z. B.; Wu, P. P.; Han, Z. W. J Mater Sci 2000, 35, 5873.
29. Wang, S. F.; Wu, P. P.; Han, Z. W. Polymer 2001, 42, 217.
30. Guo, P. Y.; Wang, S. F.; Wu, P. P.; Han, Z. W. Polymer 2004, 45, 1885.
31. Velasco-Santos, C.; Martinez-Hernandez, A. L.; Fisher, F. T.; Ruoff, R.; Castano, V. M. Chem Mater 2003, 15, 4470.
32. Zengin, H.; Zhou, W. S.; Jin, J. Y.; Czerw, R.; Smith, D. W.; Echegoyen, L.; Carroll, D. L.; Foulger, S. H.; Ballato, J. Adv Mater 2002, 14, 1480.
33. Eo, S. M.; Oh, S. J.; Tan, L. S.; Baek, J. B. Eur Polym J 2008, 44, 1603.
34. Tretiak, S.; Kilina, S.; Piryatinski, A.; Saxena, A.; Martin, R. L.; Bishop, A. R. Nano Lett 2007, 7, 86.
35. Nakayama-Ratchford, N.; Bangsaruntip, S.; Sun, X. M.; Welsher, K.; Dai, H. J. J Am Chem Soc 2007, 129, 2448.
36. Feng, L. H.; Bie, H. Y.; Chen, Z. B. J Appl Polym Sci 2005, 98, 434.